

Electronic Supplementary Information (ESI)

Solution-Processed Black Phosphorus/PCBM Hybrid Heterojunctions for Solar Cells

Linyi Bai,^a Liqun Sun,^b Yang Wang,^a Zhizhou Liu,^a Qiang Gao,^a Huijing Xiang,^a
Haiming Xie,^{*,b} and Yanli Zhao ^{*,a,c}

^aDivision of Chemistry and Biological Chemistry, School of Physical and Mathematical Sciences, Nanyang Technological University, 21 Nanyang Link, Singapore 637371

^bDepartment of Chemistry, Northeast Normal University, Changchun, Jilin 130024, PR China.

^cSchool of Materials Science and Engineering, Nanyang Technological University, 50 Nanyang Avenue, Singapore 639798

Email: xiehm136@nenu.edu.cn; zhaoyanli@ntu.edu.sg

1. Materials and instruments

All reagents and chemicals were purchased commercially and used without further purifications unless otherwise stated.

1.1 Thermogravimetric analysis (TGA) & Fourier transform infrared (FT-IR) spectra

TGA was performed on a TGA 500 thermogravimetric analyzer by heating the samples at 20 °C min⁻¹ to 1000 °C in a nitrogen atmosphere (60 mL/min). FT-IR spectra (KBr, Aldrich) were measured with a SHIMADZU IR Prestige-21 spectrometer. Samples were packed firmly to obtain transparent films.

1.2 Powder X-ray diffraction (PXRD), transmission electron microscopy (TEM) and scanning electron microscopy (SEM)

PXRD studies were performed on a SHIMADZU XRD-6000 Labx diffractometer using Cu-K α radiation at 40 kV and 300 mA with a scanning rate of 0.02° s⁻¹ (2 θ) at room temperature. TEM images were measured on a JEM-1400 (JEOL) operated at 100-120 kV. TEM grids were treated with oxygen plasma in a Harrick plasma cleaner/sterilizer for 60 s to clean the dust on the surface. The TEM grid was placed in contact with the sample solution. A filter paper was used to wick off the excess solution on the TEM grid, which was then dried in air for 30 min. SEM images were collected on a field emission JSM-6700F (JEOL) operated at 10 kV.

1.3 UV absorption and fluorescence spectra

Absorption spectra were recorded on UV-3600 UV–vis–NIR spectrophotometer (Shimadzu), while emission spectra were recorded on RF-5301 PC spectrofluorophotometer (Shimadzu) with 1.0 cm path length cell.

1.4 X-ray photoelectron spectroscopy (XPS) analysis

XPS measurements were performed with a Phiobos 100 spectrometer using Mg X-ray radiation source (SPECS, Germany) for wide range and high resolution scans at 12.53kV. The XPS samples were coated on a conductive carbon tape that was then fixed on an aluminum XPS holder.

2. Experimental details

2.1 Preparation of PCBM saturated solutions

Saturated solutions of PCBM (99.5% pure, MTR Ltd., USA) were prepared in toluene, m-xylene, chlorobenzene and CCl₄ (commercially available spectral grade solvents), respectively. The amount is ~7 mg in the respective solvent (1 mL) followed by ultrasonication for 2-3 min. In this way, PCBM powder is almost dissolved in the solvent. For an accurate control, the resulting solutions were filtered to remove undissolved PCBM to afford saturated solutions.

2.2 Selective precipitation of PCBM nanosheets

In a typical precipitation experiment, PCBM saturated CCl₄ solution (1 mL) was placed in a thoroughly cleaned and dried 10 mL glass bottle. To this bottle, t-butyl alcohol (TBA, 6 mL)

was slowly added, with temperature being maintained at 15 °C using an ice water bath during the addition. The mixture was kept at 15 °C for 15 min under ultrasonication for fully mixing. The resulting mixture was stored at room temperature in an incubator for 24 h in order to grow PCBM nanosheets.

2.3 Selective precipitation of PCBM nanowires

The PCBM powder (sigma, purity = ~ 99.5%) was mixed with m-xylene, followed by ultrasonication for 30 min. A small aliquot (~5 µL) of the final solution was dropped onto SiO₂/Si substrates, and then naturally dried under ambient conditions. The length of nanowires depends on the solvent evaporation time. For knitted nanosheets, a solvothermal reaction is necessary, in which the PCBM nanowires were transited into a fresh mixture of m-xylene and CCl₄ (v:v = 4:1), and then stored at 60 °C for 24 h to one week.

2.4 Preparation of black phosphorus (BP) dots

The micrometer-sized bulk BP crystals were synthesized from red phosphorus under high pressure and high temperature.^[S1] Despite varying the size and shape with no obvious lamellar features, the crystalline BP flakes can be obtained after 10 min sonication of bulk BP in N-methylpyrrolidinone. Then, the grinding and sonication processes were performed to exfoliate bulk BP crystals and obtain high-yield BP dots finally.

2.5 Preparation of BP-doped PCBM sheets and nanowires

For BP-doped PCBM sheets: The solution of PCBM sheets in CCl₄ was prepared firstly. Then, the as-prepared BP dots were added into the solution, followed by shaking for full mixing. The color of the dispersion was changed from dark pink to brown. Next, this mixture was stored at room temperature for 24 h. During this period, some crystals gradually formed and finally dropped on the bottom of the container. The precipitates were isolated by centrifugation, washed with CCl₄ and slight sonication for 5-10 seconds. The brown micro-size sheets can be observed under microscopy.

For BP-doped PCBM nanowires: The as-prepared BP dots were mixed with the dispersed solution of PCBM in anhydrous m-xylene followed by the ultra-sonication for 3 mins. Then, this mixture was transited into a 10 mL Schlenk storage tube (SynthwareTM, OD28 x L120mm, high vacuum valve size 0-8mm, with PTFE o-ring and wiper). Each tube was degassed by three freeze-pump-thaw cycles. Finally, each tube was sealed off, heated at 60 °C in an oven at the same time, and left undisturbed for 0-72 h. The precipitates were isolated by centrifugation, and washed with anhydrous m-xylene for 3 times, giving a purple powder with a nanowire shape.

3. Morphology modulation

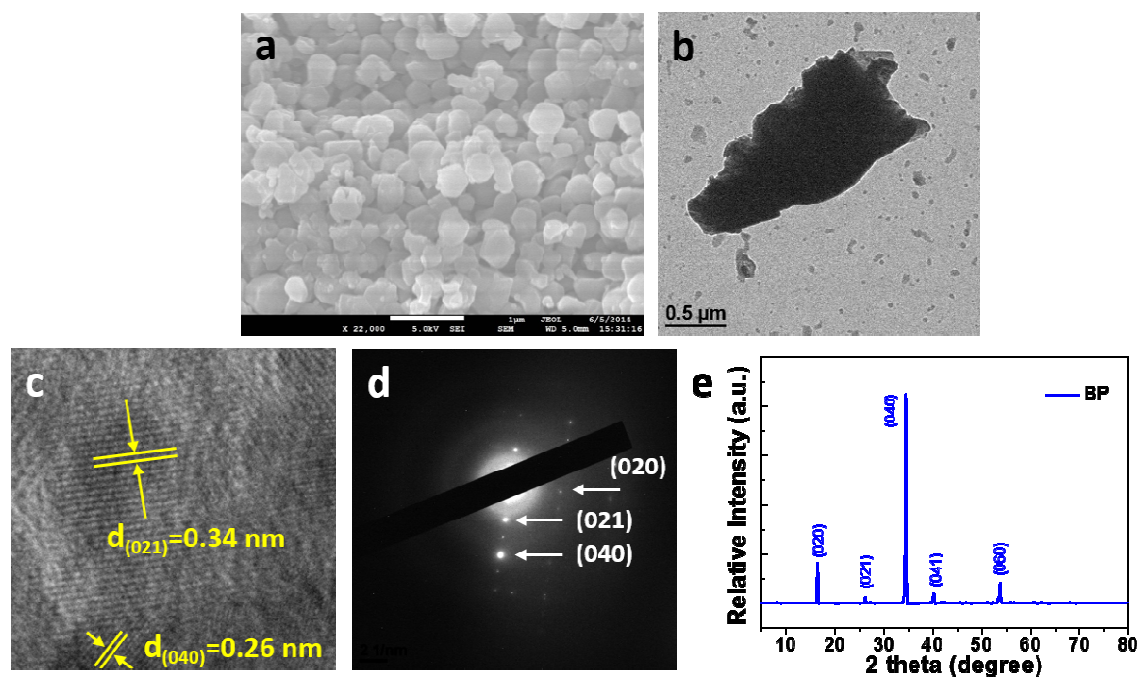


Figure S1. Characterization of bulk BP and BP flakes: (a) SEM image of bulk BP; (b) TEM image of BP flakes prepared by sonication of bulk BP in N-methyl-2-pyrrolidone for 10 min; (c) HRTEM image of BP flake; (d) SAED pattern of BP flake; (e) PXRD pattern of BP flake.

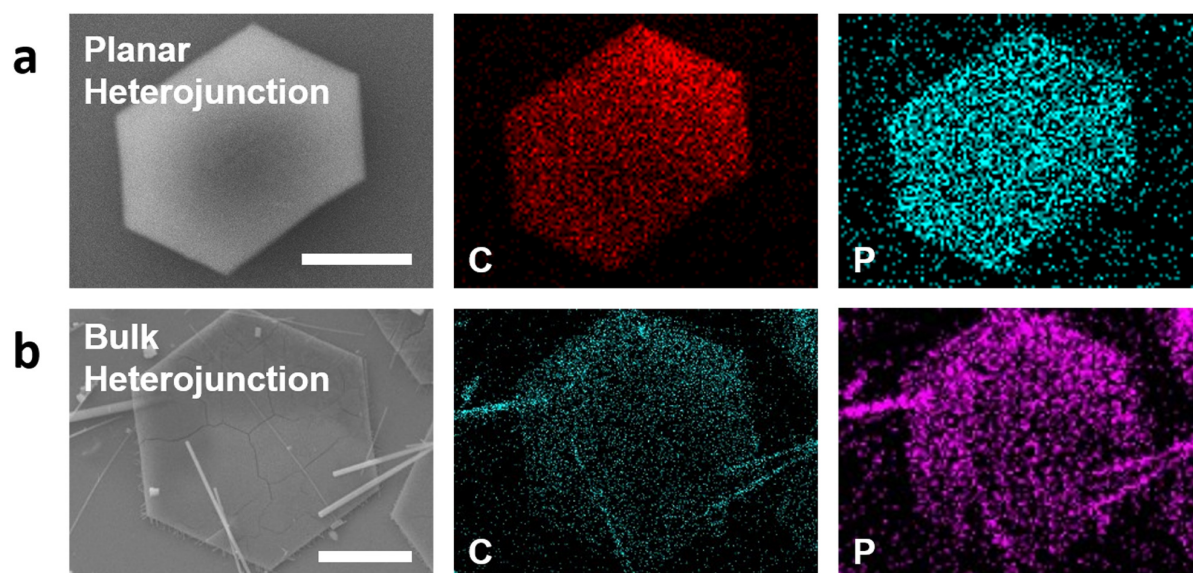


Figure S2. Elemental (C and P) mapping of (a) planar heterojunction and (b) bulk heterojunction. Scale bar: 25 μm .

Considering the solvent effect of chlorobenzene used in the device fabrications, two experiments were performed. Firstly, a saturation solution of PCBM in chlorobenzene was prepared, and the assembling process was then monitored. Although the obtained

morphology was not nice as using m-xylene, the assembly with a network shape can still be achieved (Figure S3a). In the second experiment, we directly put the assembled heterojunctions into chlorobenzene and observed any phenomenon changes. To our delight, the heterojunctions were not broken (Figure S3b,c), which should be ascribed to the protection effect of BP.

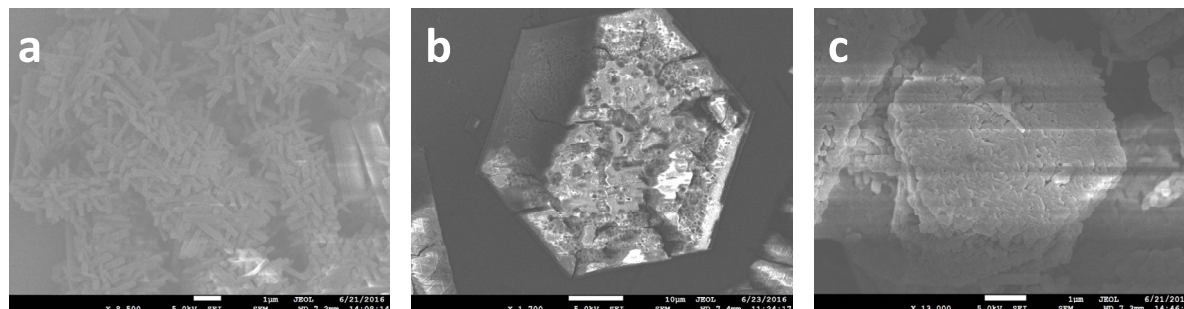


Figure S3. SEM images of (a) PCBM assemblies in chlorobenzene; (b,c) two heterojunctions of BP-PCBM in chlorobenzene treated with hand shaking.

4. Physical properties

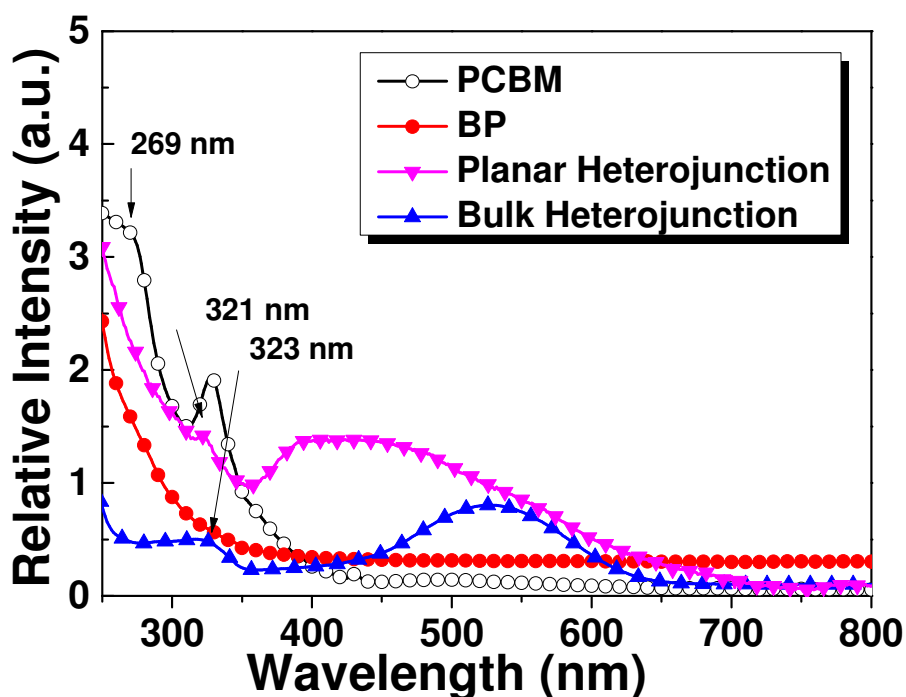


Figure S4. UV absorbance of BP, PCBM and two BP-doped PCBM hybrid heterojunctions. The samples are the dispersions of these solids with the same weight in THF.

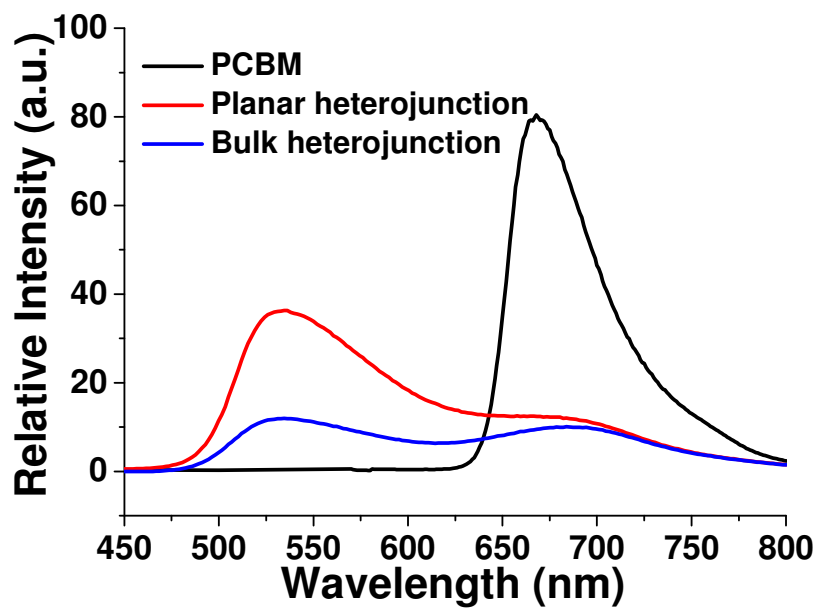


Figure S5. Solid-state fluorescence spectra of PCBM (black), planar heterojunction (red) and bulk heterojunction (blue).

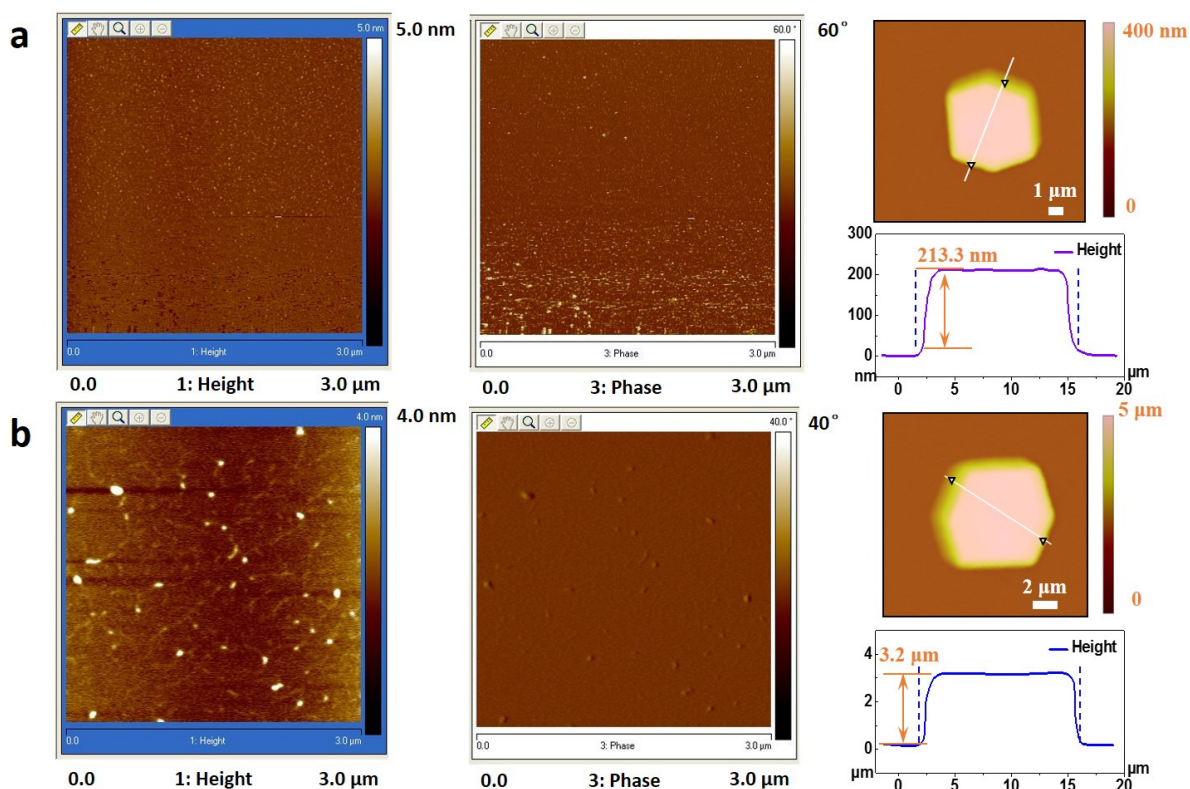


Figure S6. AFM images of two BP/PCBM heterojunctions: (a) planar heterojunction and (b) bulk heterojunction.

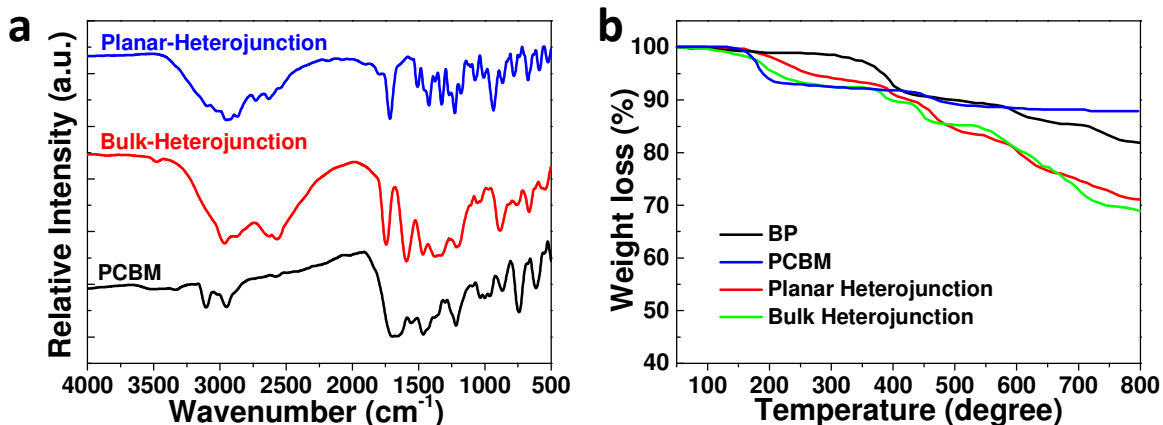


Figure S7. FT-IR spectra and TGA curves of BP, PCBM, and two hybrid heterojunctions.

5. Solar cell device fabrication

The solar cells were fabricated with the following structure: ITO-coated glass substrate / ZnO (ETL) / BP/PCBM sheets as the active layer / PEDOT:PSS (HTL) / Ag. Before the device fabrication, the ITO coated substrate was treated by separate washing in acetone, isopropanol and deionized water and then dried at 140 °C. Subsequently, ZnO used as the electron transportation layer (ETL) was spin-coated on the surface of the fore dried ITO-coated substrate under 4000 rpm, and the film thickness was ~40 nm. Then, an annealing process was performed at 75 °C for 15 min. ZnO used here was obtained by a solution-precipitation process,^[S2] where the zinc acetate solution in DMSO (0.5 M) and tetramethylammonium hydroxide (TMAH, 15 mL, 0.5 M) in ethanol were mixed and kept stirring in ambient air for 1 h. The obtained solution was centrifuged and washed with ethanol. The ZnO nanoparticles were dispersed in ethanol at a concentration of ~20 mg mL⁻¹. Next, ZnO-coated ITO substrate was transferred into a glove box to spin-cast BP/PCBM as the active layer and PEDOT:PSS as the hole transportation layer (HTL). A dichlorobenzene solution containing BP/PCBM sheets with a concentration of 20 mg/mL was spin-casted on top of the ITO under 1000 rpm. Then, PEDOT:PSS (Baytron PH) was spin-casted from aqueous solution under 4000 rpm to form a film of 40 nm thickness. After this deposition, the device was treated with the annealing at 80 °C for 10 min. It was then transferred to a vacuum chamber for Ag electrode evaporation, where a 50nm Ag electrode was deposited by thermal evaporation in a vacuum of 5×10^{-7} Torr. After the annealing, the device was placed on a metal plate to cool down at room temperature. The solar cells were masked with 0.1 cm² metal aperture to define the active area (measured individually for each mask). The optimal thickness of the device was ~2.4 mm. Current density–voltage (J–V) characteristics of the device were measured using a Keithley 236 Source Measure Unit. Solar cell performance was carried out by utilizing an Air Mass 1.5 Global (AM 1.5 G) solar simulator with an irradiation intensity of 100 W m⁻².

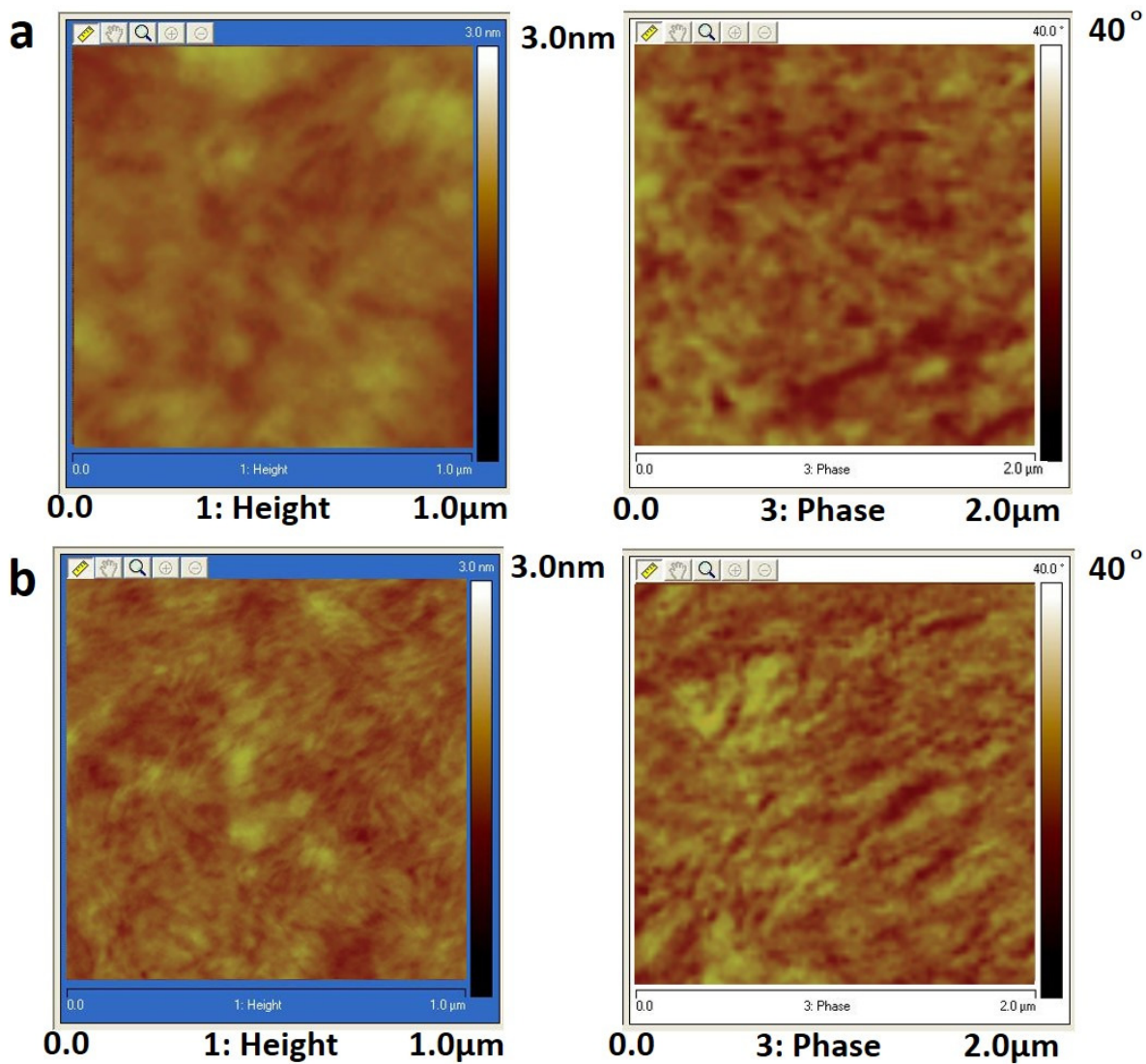


Figure S8. AFM images of two BP/PCBM hybrid heterojunction-based solar cell devices: (a) planar heterojunction and (b) bulk heterojunction.

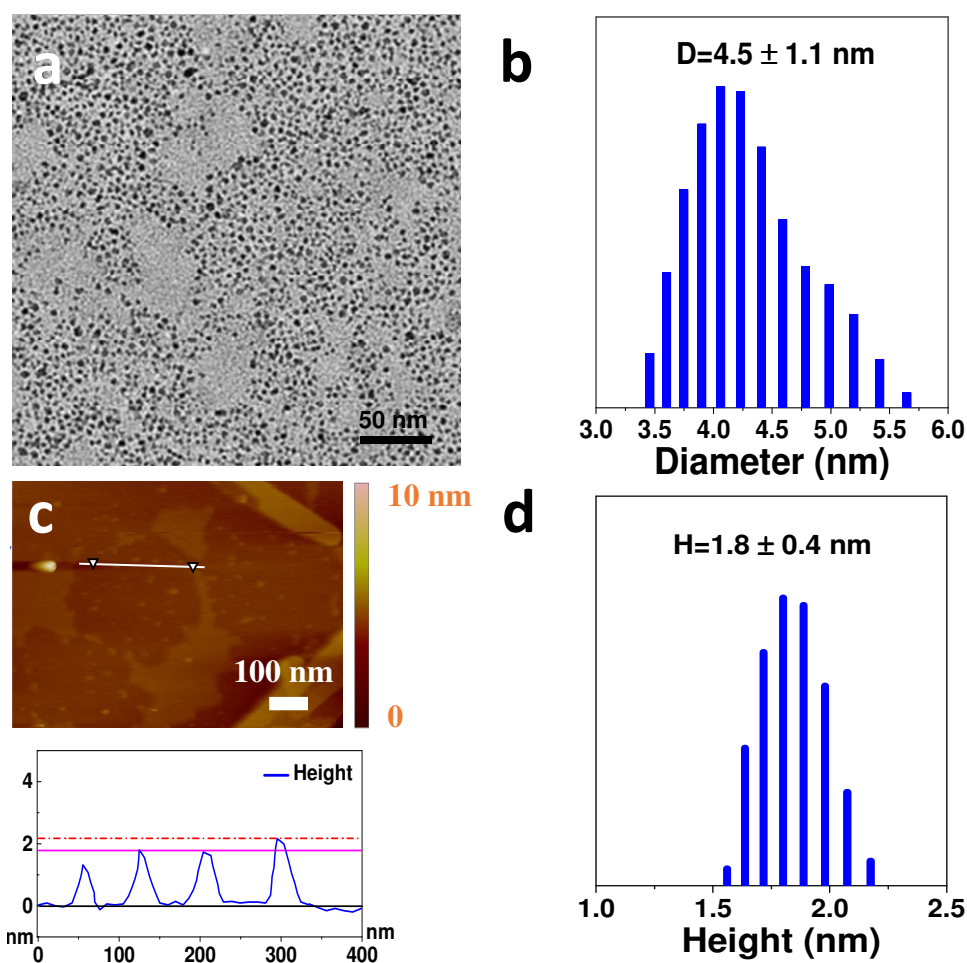


Figure S9. (a) TEM image of BP dots, (b) statistical analysis of the diameter of BP dots measured from TEM image, (c) AFM image of BP dots, and (d) statistical analysis of the height of BP dots measured from AFM image.

Table S1. Photovoltaic characteristics of the devices based on two BP/PCBM hybrid heterojunctions under annealing with the illumination of AM 1.5G 100 mW cm^{-2} .

| Devices under annealing | | J_{SC} [mA cm^{-2}] | V_{OC} [V] | FF [%] | PCE [%] |
|-------------------------|-----|----------------------------------|--------------|--------|---------|
| Planar heterojunction | 12h | 14.29 | 0.78 | 59.30 | 6.61 |
| | 24h | 14.27 | 0.78 | 58.57 | 6.52 |
| | 48h | 14.18 | 0.77 | 56.69 | 6.19 |
| | 72h | 14.13 | 0.77 | 55.97 | 6.09 |
| Bulk heterojunction | 12h | 15.92 | 0.81 | 62.50 | 8.06 |
| | 24h | 15.91 | 0.81 | 62.08 | 8.00 |
| | 48h | 15.78 | 0.81 | 60.09 | 7.68 |
| | 72h | 15.72 | 0.80 | 60.03 | 7.55 |

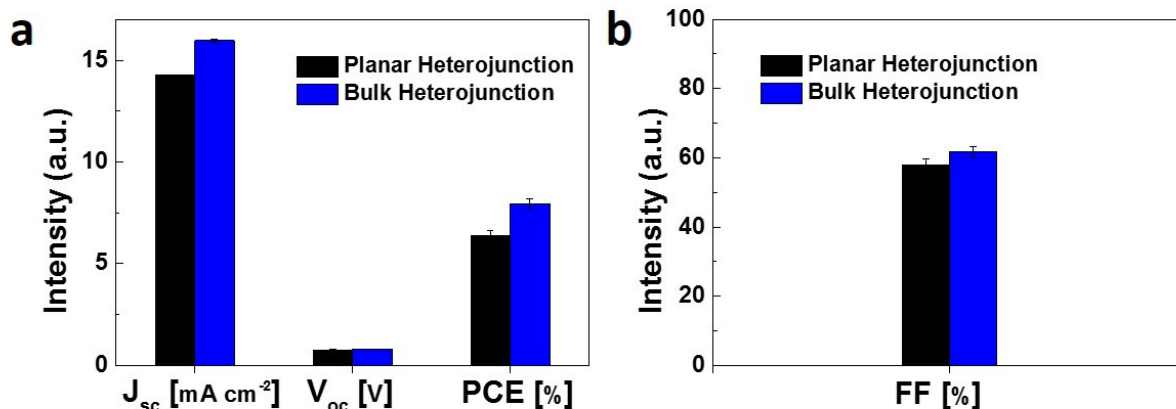


Figure S10. (a,b) Statistic standard deviation for the reproducibility of solar cell devices. The columns represent the average value and the scale bar labels mean the distribution range of each factor.

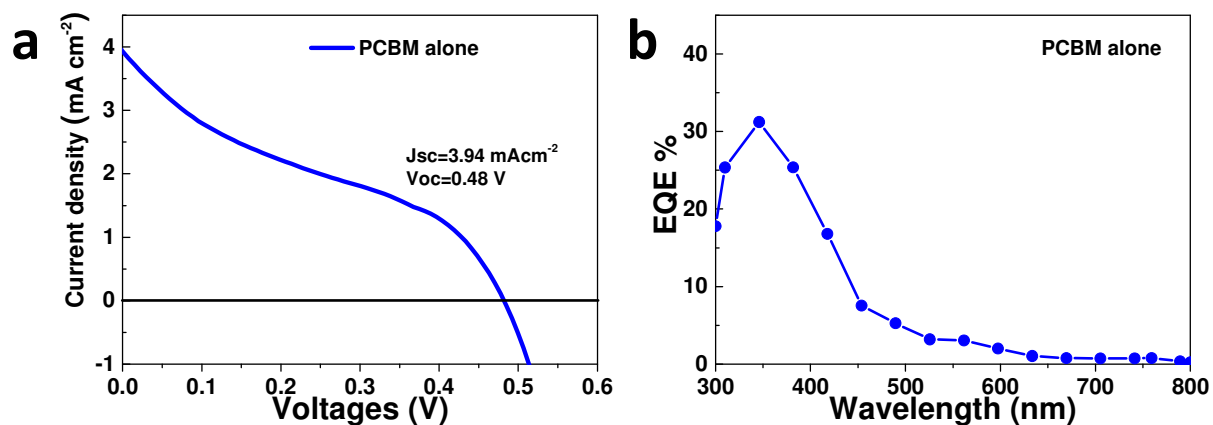


Figure S11. (a) Current intensity versus voltage and (b) EQE curve of PCBM alone.

As seen from Figure S11, the changes in current-voltage and EQE curves for PCBM alone are very obvious in comparison with BP-PCBM heterojunctions. The initial value of the current was $\sim 4 \text{ mA cm}^{-2}$, followed by a steep decrease. In the case of EQE, the conversion of PCBM was very narrow, due to its main absorbance around 350nm. Based on these comparisons, it was concluded that BP provides some contributions to the conduction and EQE in two heterojunctions.

Table S2. Photovoltaic characteristics of the devices based on two BP/PCBM hybrid heterojunctions under illumination of AM 1.5G 100 mW cm⁻².

| Devices under annealing | | J _{sc} [mA cm ⁻²] | V _{oc} [V] | FF [%] | PCE [%] |
|-------------------------|----|--|---------------------|--------|---------|
| Planar heterojunction | 1 | 14.30 | 0.78 | 60.80 | 6.80 |
| | 2 | 14.26 | 0.78 | 58.61 | 6.52 |
| | 3 | 14.24 | 0.77 | 59.37 | 6.51 |
| | 4 | 14.24 | 0.77 | 57.73 | 6.33 |
| | 5 | 14.23 | 0.77 | 56.03 | 6.14 |
| | 6 | 14.24 | 0.78 | 55.46 | 6.16 |
| | 7 | 14.26 | 0.78 | 57.45 | 6.39 |
| | 8 | 14.26 | 0.77 | 59.56 | 6.54 |
| | 9 | 14.26 | 0.77 | 55.51 | 6.07 |
| | 10 | 14.27 | 0.78 | 58.76 | 6.54 |
| Bulk heterojunction | 1 | 15.72 | 0.81 | 59.37 | 7.56 |
| | 2 | 15.95 | 0.80 | 61.36 | 7.83 |
| | 3 | 15.97 | 0.80 | 61.60 | 7.87 |
| | 4 | 16.00 | 0.81 | 62.65 | 8.12 |
| | 5 | 15.91 | 0.81 | 61.28 | 7.80 |
| | 6 | 16.02 | 0.81 | 63.35 | 8.22 |
| | 7 | 15.95 | 0.81 | 60.60 | 7.83 |
| | 8 | 16.04 | 0.81 | 64.09 | 8.30 |
| | 9 | 16.02 | 0.80 | 63.59 | 8.15 |
| | 10 | 16.00 | 0.81 | 60.73 | 7.87 |

References

- [S1] L.-Q. Sun, M.-J. Li, K. Sun, S.-H. Yu, R.-S. Wang and H.-M. Xie, *J. Phys. Chem. C*, 2012, **116**, 14772-14779.
- [S2] L. Qian, Y. Zheng, J. Xue and P. H. Holloway, *Nat. Photon.*, 2011, **5**, 543-548.